
1

General Introduction

Preface

Synaptic Transmission at the NMJ

Voltage-Gated Ca²⁺ Channels

Ca_v2.1 Channelopathies

Ca_v2.1 Channel Mutant Mice

Aims and Outline of this Thesis

Preface

Neuronal voltage-gated Ca^{2+} (Ca_v) channels play a crucial role in synaptic transmission and many other neuronal functions. Several subtypes of Ca_v channels exist, which differ in their subunit combination, kinetics, function, distribution, and their sensitivity to neurotoxins.

With the advent of modern genetic techniques in the late 1990's, the *CACNA1A* gene encoding the $\text{Ca}_v2.1$ (P/Q-type) channel has been implicated in a number of inherited neurological disorders, including Familial Hemiplegic Migraine type 1 (FHM1) and Episodic Ataxia type 2 (EA2). Similarly, the natural mouse mutants *tottering*, *leaner* and *rolling Nagoya* were found to carry mutations in the orthologous mouse gene, *Cacna1a*, accounting for their phenotypes of absence epilepsy and/or ataxia.

$\text{Ca}_v2.1$ channels are present at nerve terminals in many brain areas and at the peripheral neuromuscular junction (NMJ). Their main function is to mediate the pre-synaptic Ca^{2+} influx that stimulates neurotransmitter release. It is, therefore, likely that mutation-induced $\text{Ca}_v2.1$ dysfunction affects transmitter release, and thereby causes or contributes to the neurological disease symptoms. Furthermore, (sub-clinical) NMJ dysfunction may be present in diseases associated with $\text{Ca}_v2.1$ mutations. The NMJ is a highly specialised functional entity and the point at which the motor-axonal action potential is transduced onto the muscle fibre by synaptic transmission, and from where it is further propagated to eventually cause muscle contraction. Due to its reliance on $\text{Ca}_v2.1$ channels and the ease of experimental access, the mouse NMJ provides a valuable model to study the synaptic effects of *CACNA1A* mutations, which is the topic of this thesis.

Synaptic Transmission at the NMJ

Structure and morphology of the NMJ

Much of our knowledge of synaptic transmission today has resulted from extensive study of the NMJ (for reviews, see Sanes and Lichtman, 1999; Plomp, 2003). The NMJ is a highly specialised peripheral synapse, where the pre-synaptic neuronal action potential is transduced by chemical synaptic transmission onto the muscle fibre. There, it propagates along the post-synaptic membrane and eventually results in muscle contraction.

Myelinated axons originating from the ventral horn of the spinal cord innervate the muscle, thereby forming so-called 'motor units'. These motor units are comprised of branches of one single axon that each innervate a single muscle fibre, thus allowing one axon to innervate up to several hundred individual muscle fibres. At the point of innervation the axon branch loses its myelin sheath forming several terminal branches, which are covered by terminal Schwann cells (Figure 1).

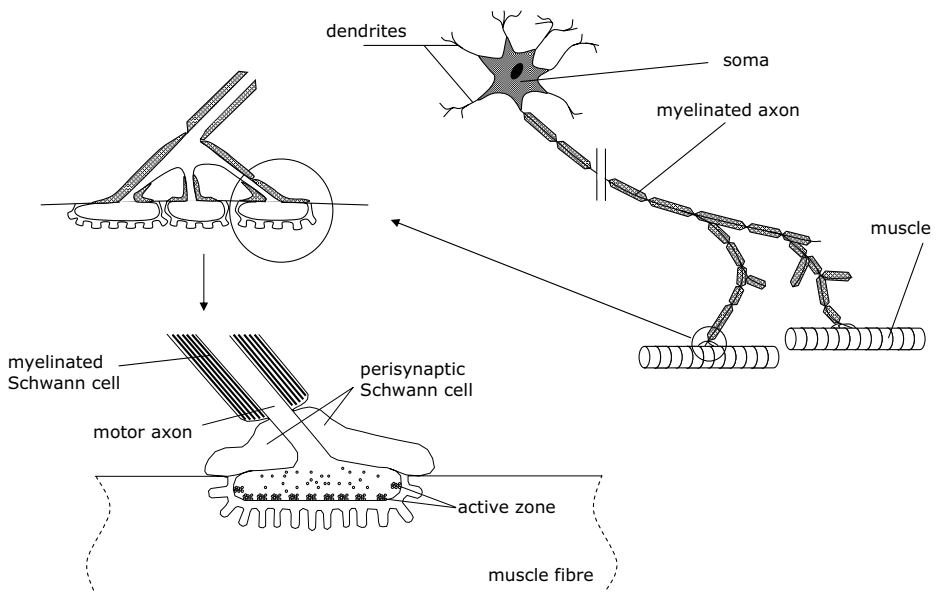


Figure 1. The neuromuscular junction (NMJ).

At the NMJ, the pre-synaptic motor nerve terminal makes contact with the post-synaptic muscle fibre. The neurotransmitter acetylcholine (ACh) is released from vesicles by fusing with the pre-synaptic membrane upon opening of pre-synaptic voltage-gated calcium channels, which provide the Ca^{2+} influx required for stimulating the release machinery. ACh binds to post-synaptic ACh receptors, opening of which results in ion flux and a transient change of membrane potential, which can be recorded using a microelectrode, and then be used to determine the amount of vesicles released per nerve impulse (quantal content). Modified from Plomp et al., 2003.

Ultrastructural analyses have revealed the structure of the pre-synaptic terminal. Clear vesicles are located in clusters at 'active zones', specialised areas at the pre-synaptic membrane. These vesicles are filled with acetylcholine (ACh), the neurotransmitter at the NMJ. Every vesicle contains one 'quantum' ACh, which consists of approximately 10,000 ACh molecules.

The post-synaptic membrane is separated from the pre-synaptic membrane by the synaptic cleft. At about 50 nm wide, the synaptic cleft contains the basal lamina that extensively covers both the muscle fibre as well as the myelinated axon branches. The basal lamina serves an important function as anchoring point for enzymes and other proteins that

are localised to the synaptic cleft (such as acetylcholinesterase, AChE). The post-synaptic membrane is organised in post-synaptic junctional folds, which provide for the differential concentration of acetylcholine receptors (AChRs) and voltage-gated Na^+ channels at the tops and bottoms of these folds, respectively, allowing the swift triggering of the post-synaptic action potential.

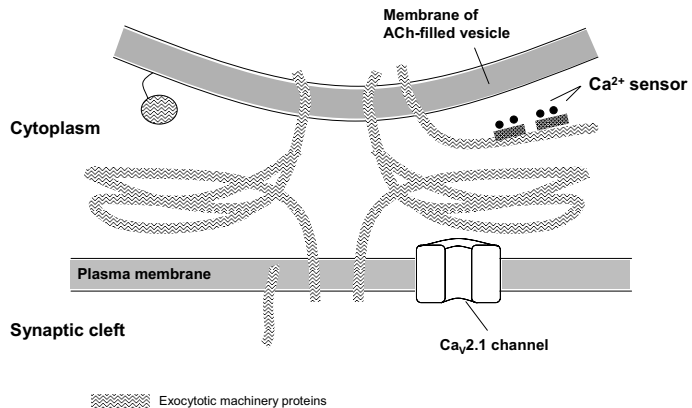
Acetylcholinergic receptors at the NMJ are of the nicotinic type (nAChRs) and are present at high density. nAChRs are heteropentameric ligand-gated ion channels containing two α - and one each of a β -, δ -, and ϵ -subunit. The NMJ (or motor endplate) is defined as the entity of the motor-nerve terminal, the synaptic cleft and the post-synaptic muscle fibre membrane enclosed by the terminal Schwann cells.

Function of the NMJ

The axonal action potential is a wave of excitation, of which the depolarising phase is caused by the opening of voltage-dependent Na^+ channels, and the repolarising phase by opening of K^+ channels. When the action potential reaches the pre-synaptic nerve terminal, the depolarisation causes $\text{Ca}_v2.1$ channels at active zones to open (Figure 2). This leads to a local influx of Ca^{2+} that subsequently triggers the release machinery and results in exocytosis of ACh-filled vesicles into the synaptic cleft. The release machinery is a highly complex functional unit of interacting proteins that by itself is the subject of intensive study (for review, see Sudhof, 2004).

Figure 2. Pre-synaptic sub-cellular localisation of $\text{Ca}_v2.1$ channels.

$\text{Ca}_v2.1$ channels are localised at active zones at the pre-synaptic membrane of motor nerve terminals. Upon voltage-gated opening of $\text{Ca}_v2.1$ channels, Ca^{2+} fluxes in and stimulates the neuro-exocytotic machinery. As a consequence, docked vesicles fuse with the membrane and release their ACh content into the synaptic cleft. Modified from Lodish et al., 2003.



Upon release of ACh into the synaptic cleft, a large proportion is immediately broken down to choline by AChE. This choline is then subjected to the ongoing process of ACh synthesis, following re-uptake into the nerve terminal.

Those molecules of ACh that successfully migrate across the synaptic cleft bind to the α subunit of nAChRs, causing the channel pore to open. This opening makes the channel permeable to the free flux of Na^+ and K^+ ions, leading to a net inward current that depolarises the post-synaptic membrane. This signal is called the endplate potential (EPP). If of sufficient amplitude, the EPP causes voltage-gated Na^+ channels to open resulting in the generation of a post-synaptic action potential. This action potential will propagate into the T-tubuli, where it will finally result in contraction of the muscle fibre.

Ex vivo electrophysiology of the NMJ

Using standard microelectrode equipment, nAChR-induced changes in post-synaptic membrane potential can be measured *ex vivo*. There are two types of depolarising events: EPPs and miniature endplate potentials (MEPPs). EPPs arise from the synchronous release of ACh

vesicles into the synaptic cleft resultant from a single nerve impulse. At the adult mouse NMJ, typical EPPs are depolarisations of ~ 25 mV. MEPPs are the result of the spontaneous unquantal release of a single vesicle of ACh. MEPPs usually occur at a frequency of ~ 0.5 - 1.5 s^{-1} , and are small depolarisations of ~ 1 mV in amplitude. The properties of EPPs and MEPPs vary even within one species and are dependent on a variety of factors, perhaps most importantly age and muscle type. As EPPs represent an additive response of unquantal events, the total number of ACh quanta released (the so-called ‘quantal content’) is an important measure of evoked ACh release, which can be calculated from the amplitudes of EPPs and MEPPs. A detailed description of the quantal content calculation is provided in chapter 3. The quantal content typically varies from 20-70, dependent on age, muscle type, and species.

Highly controlled muscle contraction is critical to any organism. This requires that every pre-synaptic action potential will result in successful muscle contraction. In order to ensure such fidelity, more ACh quanta are released from pre-synaptic active zones than strictly required to trigger a muscle action potential. This phenomenon is termed ‘safety factor’ of the NMJ (for review, see Wood and Slater, 2001).

Under normal conditions, the muscle action potential will mask the EPP and hamper stable recordings. Applying μ -conotoxin-GIIIB, a selective blocker of muscle voltage-gated Na^+ channels, prevents the generation of action potentials and enables the undisturbed recording of EPPs.

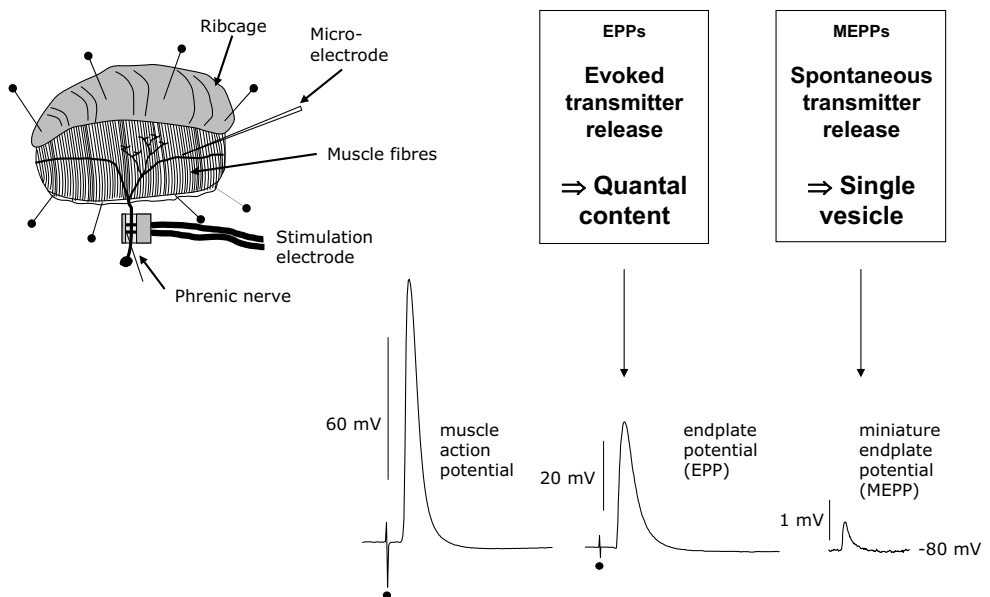


Figure 3. Schematic drawing of the mouse hemi-diaphragm/phrenic nerve preparation and electrophysiological analysis.

The phrenic nerve innervating the diaphragm is placed on a bipolar stimulation electrode. Intracellular recordings are made by impaling microelectrodes into the endplate region. Sample traces of a muscle action potential, an endplate potential (EPP) and a miniature endplate potential (MEPP) are shown. The number of vesicles emptied per nerve stimulus (quantal content) can be calculated by dividing the EPP amplitude by the MEPP amplitude (cf. Methods described in chapter 3, page 50).

The muscle-nerve preparation of choice for most studies described here is the diaphragm-phrenic nerve preparation (Figure 3). Several properties make this particular preparation highly suitable for microelectrode recordings. Firstly, the diaphragm of the mouse is a flat and thin (only about 10 fibre layers-thick) muscle, allowing it to be pinned out effectively and providing good visibility of individual muscle fibres. Secondly, the phrenic nerve

innervating the diaphragm forms a well-defined and easily identifiable NMJ region, allowing precise impaling with the microelectrode. Lastly, the phrenic nerve can be dissected to a length sufficient to be placed over a bipolar stimulus electrode thus circumventing the use of a suction electrode, which is technically more challenging and mostly associated with larger stimulus artefacts due to the higher stimulation voltages required and closer proximity of the stimulus- and the recording electrode.

The diaphragm-phrenic nerve preparation is pinned out in a 30 mm rubbersilica-coated dish, and the phrenic nerve placed on a bipolar stimulus electrode and well insulated with Vaseline, before the dish is filled with physiological Ringer's medium.

Using a glass micro-electrode (filled with 3 M KCl solution, with a tip of $\sim 1 \mu\text{m}$ in diameter and a resistance of $\sim 15 \text{ k}\Omega$, connected to an amplifier) and a bath reference electrode, the so-called resting membrane potential can be recorded after impaling the micro-electrode into a muscle fibre. EPPs and MEPPs can thus be measured upon ACh release from the pre-synaptic nerve terminal. The analogue signals are digitised and stored on a computer, before they are analysed off-line, following the completion of the experiments.

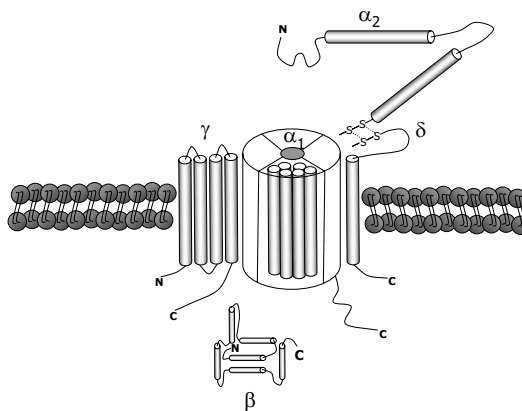


Figure 4. Structure of voltage-gated Ca^{2+} channels.

Voltage-gated Ca^{2+} channels consist of the channel-forming α_1 subunit, the dimeric $\alpha_2\delta$ subunit, an intracellular phosphorylated β subunit and a transmembrane γ subunit.

Voltage-Gated Ca^{2+} Channels

Ca_v channels belong to the superfamily of voltage-gated ion channels sharing common 'ancestors' with voltage-gated K^+ and Na^+ channels. Ca_v channels open upon membrane depolarisation (e.g. action potentials) and mediate inward Ca^{2+} influx.

Initially purified from transverse tubules of skeletal muscle (Curtis and Catterall, 1984), biochemical analysis of the various components soon gave rise to the paradigm that Ca^{2+} channels consist of four subunits: a pore-forming α_1 subunit of 190 kDa, a 170 kDa dimer ($\alpha_2\delta$) that is linked together via a disulphide bridge, an intracellular phosphorylated β subunit of 55 kDa, and a transmembrane subunit (33 kDa) designated γ (Takahashi et al., 1987; Figure 4).

Subsequently, various other channels consisting of highly homologous channel-forming subunits were identified that exhibit distinct pharmacological profiles, kinetics and very different sensitivities to neurotoxins and drugs (Figure 5; Table 1; for review, see Doering and Zamponi, 2003).

Separate alphabetical nomenclatures evolved for describing channel types according to their distribution and kinetics, and to the different α_1 subunits identified, respectively. However, with an increasing number of new Ca^{2+} channel types and isoforms being cloned, this

system had become ambiguous and confusing. Since then several attempts have been made to adopt a new more systematic nomenclature that accounts for the phylogeny of Ca^{2+} channels (Ertel et al., 2000), similar to the one used (so far successfully) for describing K^{+} channels. An outline of this new systematic nomenclature of Ca_v channels is given in Table 1 and will be used throughout this thesis.

Ca_v channels are sub-divided in the classes of high voltage-activated (HVA) and low voltage-activated (LVA) channels. The group of HVA channels consists of Ca_v1 (L-type), $\text{Ca}_v2.1$ (P/Q-type), $\text{Ca}_v2.2$ (N-type) and $\text{Ca}_v2.3$ (R-type) channels, whereas the group of LVA channels is constituted of Ca_v3 (T-type) channels (see also Table 1).

Functional diversity of Ca_v channels is not limited to subunits encoded by different genes, but is also conferred by alternative splicing of a single gene. Alternative splicing has been reported for all known types of HVA Ca^{2+} channels, especially the α_1 subunit (for review, see Lipscombe et al., 2002). Together with a function-specific distribution and assembly/interaction with accessory subunits or other proteins, the wide range of HVA Ca^{2+} channel combinations which are possible, have the ability to fulfil a plethora of highly specialised functions. These include mediation of neurotransmission, gene expression and synaptic plasticity.

Genes encoding Ca_v channels are implicated in a large number of human disorders, including neurological and pain disorders, as well multi-organ diseases (such as Timothy's syndrome). The present thesis focuses on CACNA1A-encoded $\text{Ca}_v2.1$ channels, which are located on cell bodies and pre-synaptic terminals (Westenbroek et al., 1995; Westenbroek et al., 1998), where they govern neurotransmitter release both in the central (CNS) and peripheral nervous system (PNS). In the CNS, different cell types utilise varying degrees of $\text{Ca}_v2.1$ channel involvement in neurotransmitter release. For instance, cerebellar Purkinje cells (PCs) are dependent on more than 90% of their Ca^{2+} influx occurring through $\text{Ca}_v2.1$ channels (Mintz et al., 1992ab), compared with only approximately 50% in cerebellar granule cells (CGCs; Mintz et al., 1995). Neuromuscular synaptic transmission is exclusively dependent on $\text{Ca}_v2.1$ channels for ACh release (Uchitel et al., 1992; this thesis). In the following I shall concentrate on disorders caused by aberrant $\text{Ca}_v2.1$ channel function.

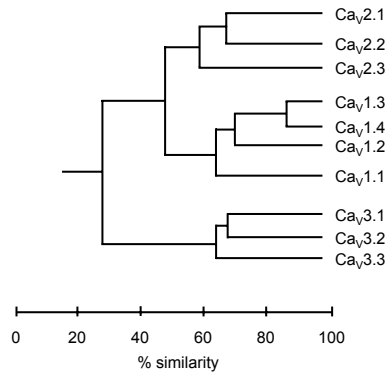


Figure 5. Protein sequence similarity of mammalian pore-forming Ca_v channel subunits; modified from Snutch et al., 2005.

Ca^{2+} Channel	Ca^{2+} Current	Name α_1 -subunit	Gene	Specific blocker(s)
$\text{Ca}_v1.1$	L-type	α_{1S}	CACNA1S	Dihydropyridines, benzothiazapines, phenylalkylamines
$\text{Ca}_v1.2$		α_{1C}	CACNA1C	
$\text{Ca}_v1.3$		α_{1D}	CACNA1D	
$\text{Ca}_v1.4$		α_{1F}	CACNA1F	
$\text{Ca}_v2.1$	P/Q-type	α_{1A}	CACNA1A	ω -Agatoxin-IVA, ω -Conotoxin-MV1IC
$\text{Ca}_v2.2$	N-type	α_{1B}	CACNA1B	ω -Conotoxin-GVIA, ω -Conotoxin-MV1IC
$\text{Ca}_v2.3$	R-type	α_{1E}	CACNA1E	SNX-482
$\text{Ca}_v3.1$	T-type	α_{1G}	CACNA1G	Mibefradil, kurtoxin, amiloride
$\text{Ca}_v3.2$		α_{1H}	CACNA1H	
$\text{Ca}_v3.3$		α_{1I}	CACNA1I	

Table 1. Nomenclature of voltage-gated Ca^{2+} channels according to Ertel et al., 2000.

Ca_v2.1 Channelopathies

The list of known disorders resulting from Ca²⁺ channel dysfunction (Ca²⁺ channelopathies) includes a number of neurological conditions with underlying Ca_v2.1 channel dysfunction. These can either be inherited diseases caused by mutations in the CACNA1A gene, or diseases of auto-immune origin. CACNA1A mutations have been shown to cause a severe subtype of hereditary migraine, episodic and spinocerebellar ataxias, and rare forms of epilepsy (Ophoff et al., 1996; Zhuchenko et al., 1997; Jouvenceau et al., 2001; Imbrici et al., 2004; see also Figure 6). In Lambert-Eaton myasthenic syndrome (LEMS), auto-antibodies target Ca_v2.1 channels causing severe functional impairment of neuromuscular synaptic transmission leading to muscle weakness (Kim and Neher, 1988). In the following, I shall present these Ca_v2.1 channelopathies in more detail, before focusing on the various mouse models that were employed in the experiments described in this thesis.

Familial Hemiplegic Migraine (FHM)

Typical migraine is a headache disorder of paroxysmal nature. Affecting approximately 6% of males and up to 18% of females, migraine is listed by the World Health Organization in the highest class of the most disabling disorders.

“What is undisputed is that migraine and tension-type headache are the most prevalent disorders and, both with disabling potential, they have the greatest impact on public health. ... [They] impose a significant health burden, with nearly all migraine sufferers [...] experiencing reductions in social activities and work capacity. Despite this, both the public and health care professionals tend to perceive headache as a minor or trivial complaint. As a result, the physical, emotional, social and economic burdens of headache are poorly acknowledged in comparison with those of other, less prevalent, disorders.”

(World Health Organization, 2000)

Available pharmacotherapies are often unsatisfactory (Goadsby et al., 2002), and currently are mostly limited to pain relief rather than causal treatment or prophylaxis. Furthermore, no marker for migraine has so far been identified, despite a clearly established partial genetic involvement (Pietrobon, 2005a). Diagnosis thus, has to rely on patient history and be based upon the classification of headache disorders as drawn up by the International Headache Society (The International Headache Society, 2004).

Migraine can be divided into two major sub-types. Whereas migraine without aura (MO) is a clinical syndrome characterised by headache with autonomous symptoms such as phono- and photophobia and nausea, migraine with aura (MA) is primarily characterised by the visual and/or auditory hallucinatory aura symptoms that usually precede the headache (The International Headache Society, 2004).

A process termed “cortical spreading depression” (CSD) is thought to underlie the migraine aura (Olesen et al., 1981; Lauritzen, 1994) and considered an event that precedes the headache attack (Pietrobon, 2005a). CSD is a slowly propagating wave of strong neuronal depolarization that causes transient intense spike activity, followed by long-lasting neuronal silence (Lauritzen, 1994; Pietrobon, 2005a).

Familial hemiplegic migraine (FHM) is an inherited severe form of MA (OMIM #141500) characterised by ictal hemiparesis during the migraine attack. Due to its monogenic inheritance and similarity to MA, FHM is considered a useful model to gain further insights into the pathophysiology of typical migraine (Pietrobon and Striessnig, 2003). To date, mutations in three different genes have been shown associated with FHM (Ophoff et

al., 1996; Vanmolkot et al., 2003; De Fusco et al., 2003; Dichgans et al., 2005), forming the basis for the current FHM classification:

- FHM1: mutations in *CACNA1A*, coding for the pore-forming subunit of neuronal voltage-gated $\text{Ca}_v2.1$ Ca^{2+} channels;
- FHM2: mutations in *ATP1A2*, coding for the α_2 subunit of the Na^+/K^+ -ATPase;
- FHM3: mutations in *SCN1A*, coding for a neuronal voltage-gated Na^+ channel.

To date, nearly 20 distinct FHM1 mutations have been identified, differing significantly in their prevalence and the severity of the clinical symptoms associated with them. Many of these mutations have been studied in detail in heterologous expression systems, including transfected human embryonic kidney (HEK) cells (Kraus et al., 1998; Hans et al., 1999; Tottene et al., 2002; Melliti et al., 2003; Mullner et al., 2004; Cao et al., 2004; Barrett et al., 2005; Cao and Tsien, 2005; Tottene et al., 2005).

Whole-cell voltage-clamp measurements have suggested a common property among several FHM1 mutations, namely a shift in activation voltage of the channel in the negative direction (for review, see Pietrobon and Striessnig, 2003). This shift predicts opening of mutated $\text{Ca}_v2.1$ channels as a result of depolarisations that would cause native channels to remain closed. Such a common effect suggests increased influx of Ca^{2+} through these channels into the pre-synaptic terminal, resulting in increased neurotransmitter release.

Conflicting reports exist regarding the effects on Ca^{2+} current density of mutations in $\text{Ca}_v2.1$ channels, suggesting either increase (Hans et al., 1999) or reduction (Cao et al., 2004). Different experimental settings and the use of different expression systems may account for these discrepancies, however. These findings have highlighted the need for animal models that allow the study of mutated $\text{Ca}_v2.1$ channels in their native (pre-synaptic) environment. Chapters 2 - 4 describe the generation and characterisation of two novel *Cacna1a* knock-in (KI) mutant mouse strains, carrying the FHM1 mutations R192Q and S218L (Figure 6; cf. section on $\text{Ca}_v2.1$ Mutant Mice, page 21). Their usefulness in the elucidation of FHM1 pathophysiology is discussed.

Episodic ataxia type 2 (EA2)

Caused by mutations in *CACNA1A* (Ophoff et al., 1996), EA2 manifests as paroxysmal attacks with a broad spectrum of severity, ranging from mild to very severe episodes depending on the mutation. This phenomenon is termed ‘allelic heterogeneity’. Typically, EA2 symptoms include ataxia, nystagmus, dysarthria, vertigo, diplopia and general weakness. Attacks last from minutes to days, in rare cases, however, symptoms can prevail several days. Stress (both emotional and physical) is the most important trigger of EA2. First symptoms usually appear during late childhood or adolescence. Interictal cerebellar symptoms are common and can include down-beat nystagmus or mild gait ataxia and tend to be mildly progressive.

Expression of human EA2 mutations in transfected cells lines have shown that most mutations result in severely truncated dysfunctional or non-functional $\text{Ca}_v2.1$ channels. Recently, some mutations have been identified which result in single amino acid changes, located in close proximity to the S5-S6 linkers of $\text{Ca}_v2.1$. Their location is thought to critically interfere with channel gating. The neurological symptoms of EA2 are thought to result from dominant-negative effects of these EA2 mutations on (cerebellar) neurotransmission (Jeng et al., 2006). Besides the CNS symptoms, neuromuscular abnormalities have been identified in EA2 mutations, causing ‘jitter’ and block of neurotransmission as assessed by single-fibre electromyography (EMG) (Jen et al., 2001).

EA2 is treated with acetazolamide, which is effective in more than 90% of all cases. The precise mechanism of action of acetazolamide has not been established to date. EAs have been comprehensively reviewed elsewhere (Kullmann, 2002; Pietrobon, 2002; Herrmann et al., 2005).

Chapter 9 assesses the use of heterozygous *Cacna1a-leaner* and heterozygous $\text{Ca}_v2.1$ -knock-out (KO) mice as models for EA2 and studies the possible effects of acetazolamide on ACh release at the mouse NMJ.

Spinocerebellar ataxia type 6 (SCA6)

SCA6 belongs to the group of autosomal dominant cerebellar ataxias, and is a late-onset slowly progressive cerebellar ataxia. Episodes are variable in frequency (from yearly to daily), and in duration (from seconds to days). Characteristic symptoms of SCA6 attacks include nystagmus, dysarthria, dysphagia, and vibratory and proprioceptive sensory loss, and show broad phenotypical overlap with EA2 (Zhuchenko et al., 1997; for review, see Mantuano et al., 2004).

SCA6 is caused by an expansion of a poly-glutamine stretch in the C-terminal region of the $\text{Ca}_v2.1$ channel. Whereas the normal stretch size varies between four and 18 units, SCA6 patients have 20 - 30 glutamine units (Zhuchenko et al., 1997; for review, see Mantuano et al., 2004).

Poly-glutamine stretches can form toxic aggregates, such as those aetiologic in the pathophysiologies of Huntington's disease or spinal and bulbar muscular atrophy. For SCA6, aggregate formation has been demonstrated in cultured PCs (Ishikawa et al., 1999; Ishikawa et al., 2001), suggesting that poly-glutamine toxicity may play a role in SCA6 pathophysiology. This hypothesis is supported by dramatically increased current density of SCA6-mutated $\text{Ca}_v2.1$ channels found in transfected cells (Piedras-Renteria et al., 2001). However, another study showed normal current density accompanied by a negative shift in the voltage-dependence of inactivation (Matsuyama et al., 1999; Toru et al., 2000). The extent of this shift was dependent on the number of glutamine repeats (Toru et al., 2000). Restituito et al. (2000) found very different effects on the biophysical properties of SCA6- $\text{Ca}_v2.1$ channels in *Xenopus* oocytes, compared to the other studies, namely increased Ca^{2+} influx and a reduced rate of inactivation. In SCA6 patients, no NMJ dysfunction, as assessed by EMG, was observed (Jen et al., 2001; Schelhaas et al., 2004). More insights into the regulation of expression of the wild-type $\text{Ca}_v2.1$ channel and into the synaptic effects of poly-glutamine stretches are required for a better understanding of the contributing factors in SCA6 pathophysiology.

Lambert-Eaton myasthenic syndrome (LEMS)

LEMS is a paraneoplastic disorder characterised by muscle weakness, impaired tendon reflexes and autonomic dysfunction. In around 60% of patients, LEMS is associated with small-cell lung cancer of neuroendocrine origin that can often only be diagnosed several years after onset of the neurological symptoms (O'Neill et al., 1988).

Auto-antibodies directed against $\text{Ca}_v2.1$ Ca^{2+} channels have been identified as the underlying cause in LEMS (Kim and Neher, 1988). At the NMJ these antibodies block or eliminate their channel targets, thereby reducing Ca^{2+} influx into the pre-synaptic terminal, which results in a decreased number of ACh quanta released upon nerve impulses (Lambert and Elmqvist, 1971). It has furthermore been shown that anti- $\text{Ca}_v2.1$ Ca^{2+} channel antibodies are capable of down-regulating transmitter release from sympathetic and parasympathetic neurones (Waterman et al., 1997), thereby causing the autonomic dysfunction observed in LEMS patients.

Initial diagnosis of LEMS relies on EMG abnormalities: a decrementing compound muscle action potential (CMAP) response to low-frequency nerve stimulation in the hand, and an initial low CMAP amplitude. These EMG abnormalities are observed also in another NMJ disorder, myasthenia gravis, where post-synaptic nAChRs are autoimmune targets). However, post-tetanic facilitation (i.e. increase in CMAP amplitude of at least 100%) is considered to be unique to LEMS (AAEM Quality Assurance Committee, 2001). Subsequent to positive EMG diagnosis, screening of serum samples for $\text{Ca}_v2.1$ Ca^{2+} channel-specific antibodies usually provides final confirmation of the diagnosis.

The typical treatment regime for LEMS consists of 3,4-diaminopyridine, a blocker of voltage-gated K^+ channels, which causes prolongation of nerve action potentials resulting in an increase in opening time of the remaining available $\text{Ca}_v2.1$ channels. The subsequent increase in pre-synaptic Ca^{2+} influx causes a larger release of ACh quanta, thereby compensating for the loss of functional $\text{Ca}_v2.1$ channels.

Despite a lack of clear clinical evidence, many patients report an alleviation of symptoms when the treatment regime is extended to administration of pyridostigmine in addition to 3,4-diaminopyridine. Pyridostigmine is an AChE inhibitor, which is commonly used in treating myasthenia gravis. By reducing the rate of ACh cleavage in the synaptic cleft, it increases the post-synaptic availability of ACh, thereby enhancing neuromuscular synaptic transmission.

$\text{Ca}_v2.1$ Channel Mutant Mice

Several mouse models exist that carry mutations in either the pore-forming *Cacna1a*-encoded $\text{Ca}_v2.1$ - α_1 protein, or the accessory subunits (for review, see Pietrobon, 2005b). I shall restrict myself in the following exposition, however, to those model strains that have been employed in the work described in the present thesis.

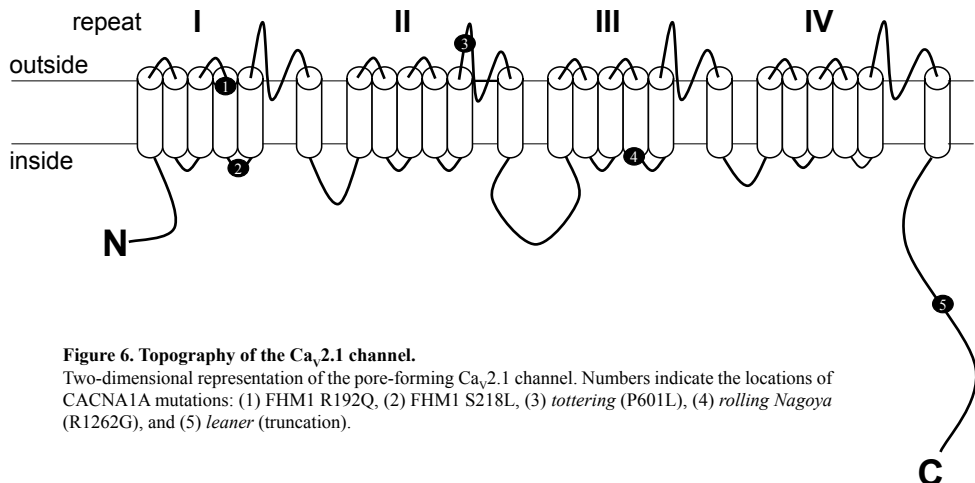


Figure 6. Topography of the $\text{Ca}_v2.1$ channel.

Two-dimensional representation of the pore-forming $\text{Ca}_v2.1$ channel. Numbers indicate the locations of CACNA1A mutations: (1) FHM1 R192Q, (2) FHM1 S218L, (3) *tottering* (P601L), (4) *rolling Nagoya* (R1262G), and (5) *leaner* (truncation).

Tottering

The natural mouse mutant *tottering* is a long-known model for human absence epilepsy, discovered some 45 years ago (Green and Sidman, 1962). The *tottering* locus was eventually mapped to the *Cacna1a* gene, encoding $\text{Ca}_v2.1$ channels (Fletcher et al., 1996; Doyle et al., 1997; Figure 6).

Tottering mice exhibit a delayed-onset neurological phenotype, which has proven difficult to dissect, and has not been completely elucidated to date. Ataxia is manifested around postnatal day (P) 21 by a hopping gait and the tail frequently arched over the back. Furthermore, *tottering* mice suffer from dystonia and spike-wave discharges on electroencephalogram recordings, characteristic of human absence epilepsy (Kaplan et al., 1979; Noebels and Sidman, 1979). The convulsive seizures (intermittent myoclonus) of *tottering* mice are not associated with electroencephalographic changes (Le Gal and Naquet, 1990).

Tottering brains seem cytoarchitecturally normal, except for extensive hyperinnervation of the axons of the locus ceruleus (Levitt and Noebels, 1981) causing the observed spike-wave discharges (Noebels, 1984). In wild-type mice, the enzyme tyrosine hydroxylase is transiently expressed in cerebellar PCs during development (P21-35). In *tottering* mice, however, expression persists through adulthood (Hess and Wilson, 1991; Austin et al., 1992). Ca_v1 channels are up-regulated in cerebellar PCs, possibly as compensatory response to ectopic tyrosine hydroxylase expression (Campbell and Hess, 1999). This Ca_v1 channel up-regulation appears responsible for the episodes of dystonia in *tottering* mice as dihydropyridines, selective Ca_v1 channel blockers, can prevent restraint-induced motor epilepsy episodes (Campbell and Hess, 1999). Conversely, the Ca_v1 agonist Bay K8644 initiated seizures at lower concentrations than needed in wild-type. Furthermore, when bred on the *Purkinje cell degeneration* background, *tottering* mice do not exhibit dystonia (Campbell et al., 1999).

The underlying mechanisms that cause ataxia in *tottering* mice have not been unequivocally determined. An altered γ -aminobutyric acid type-A (GABA_A) receptor profile in *tottering* CGCs may, however, contribute to the aetiology of ataxia (Kaja et al., 2003).

Electrophysiological analysis revealed that whole-cell current density and voltage-dependent inactivation are reduced in *tottering* dissociated cerebellar PC somata (Wakamori et al., 1998). In their synaptic study on *tottering* hippocampal cells, Qian and Noebels (2000) found that Ca^{2+} influx through *tottering*-mutated $\text{Ca}_v2.1$ channels is drastically reduced. Furthermore, $\text{Ca}_v2.2$ channels compensate for *tottering*-mutated $\text{Ca}_v2.1$ channels. In thalamic neurones, evoked excitatory post-synaptic currents (EPSCs) were reduced in *tottering* brain, whereas inhibitory post-synaptic currents (IPSCs) were indistinguishable from wild-type (Caddick et al., 1999). In contrast, peak current densities of LVA Ca^{2+} currents were increased by nearly 50% in thalamocortical slices of *tottering* mice, without alteration in the expression levels of mRNA of the three genes encoding LVA Ca_v3 channel subunits (Zhang et al., 2002).

Analysis of the NMJ of *tottering* mice revealed an increased spontaneous ACh release, whereas low-rate evoked release was at normal levels (Plomp et al., 2000). However, high-rate evoked ACh release was mildly reduced. In muscle contraction experiments, neuromuscular transmission of *tottering* mice appeared more sensitive to D-tubocurarine, indicating a reduced safety factor (Plomp et al., 2000). Furthermore, ACh release appeared to be slightly less sensitive to the selective $\text{Ca}_v2.1$ channel blocker ω -agatoxin-IVA, suggesting functional compensation by other types of Ca_v channels. In chapter 5 this hypothesis is investigated using several Ca_v channel subtype-specific blocking toxins.

Rolling Nagoya

Rolling Nagoya mice are natural *Cacnala* mutants, carrying a R1261G point-mutation (Mori et al., 2000; Figure 6). They present with severe ataxia that causes the animal to roll to the side, hence the name. The ataxia is more severe than in *tottering* mice, but motor seizures are not present in *rolling Nagoya* mice (Oda, 1973). One similarity with *tottering* mice is the persistent expression of tyrosine hydroxylase in cerebellar PCs (Sawada et al., 1999).

However, ectopic tyrosine hydroxylase expression does not contribute to the neurological phenotype of *rolling Nagoya*. Controversy has arisen over the presence of morphological abnormalities, atrophy and apoptosis present in *rolling Nagoya* mice. The presence of ectopic dendritic PC spines similarly to *tottering*, has been reported (Rhyu et al., 1999a; Rhyu et al., 1999b). Up to seven synaptic connections between a single parallel fibre varicosity with different PC dendritic spines were found in the *rolling Nagoya* cerebellum, whereas normal asymmetric synapses consist of a single pre-synaptic varicosity and one, or occasionally two PC dendritic spines (Rhyu et al., 1999a). *Rolling Nagoya* mice also showed severe CGC loss and CGCs undergoing apoptosis, identified on the basis of condensed CGC nuclei and TUNEL staining (Rhyu et al., 1999b; Suh et al., 2002). In contrast, Mori et al. (2000) reported normal cerebellar morphology.

Electrophysiological measurements of heterologously expressed *rolling Nagoya*-mutated $Ca_v2.1$ channels revealed a shift of the activation voltage of the mutated channel in the positive direction, and a reduction of the steepness of the curve (Mori et al., 2000). Similar changes have also been reported for native *rolling Nagoya* channels in cerebellar PCs (Mori et al., 2000). Besides this change in the voltage dependence of activation, native channels also showed a shift in voltage dependence of the inactivating component towards less negative values (Mori et al., 2000). In the only synaptic study to date, strikingly opposing effects of the *rolling Nagoya* mutation were found at different cerebellar synapses: EPSC amplitudes were decreased in parallel fibre synapses, but increased in climbing fibre synapses (Matsushita et al., 2002). Chapter 6 provides a detailed characterisation of neuromuscular synaptic transmission in *rolling Nagoya* mice.

Leaner

The *leaner* mutation is located in a splice-donor consensus region, yielding two possible isoforms of the protein that both lack the C-terminal region (designated 'long' and 'short'; Figure 6) (Fletcher et al., 1996; Doyle et al., 1997). The short isoform gave rise to a significantly reduced current density, whereas the long isoform showed a positive shift in activation voltage (Dove et al., 1998; Lorenzon et al., 1998; Wakamori et al., 1998). It has, therefore, been suggested that the C-terminus is required for normal channel-gating (Dove et al., 1998). In *leaner* channel gating is reduced, whereas both the macroscopic channel properties and their sensitivity to neurotoxins remain unaltered (Dove et al., 1998). No changes in either mRNA or protein expression have been reported for *leaner* cerebellum (Lau et al., 1998).

Homozygous *leaner* mice show a phenotype of severely progressive ataxia, cortical spike-wave discharges and premature death, typically during the fourth postnatal week. Furthermore, PCs are reduced by approximately 80% (Herrup and Wilczynski, 1982), those remaining show abnormal morphology (Heckroth and Abbott, 1994). Several findings in *leaner* mice hint towards slower development, such as the persistent expression of the enzyme tyrosine hydroxylase (Hess and Wilson, 1991; Austin et al., 1992), reduced Ca^{2+} buffering capacity of PC neurones (Dove et al., 2000) and PC morphology (Rhyu et al., 1999a). However, the exact mechanisms by which changes in $Ca_v2.1$ channel function lead to the *leaner* phenotype remain unsolved to date. In chapter 7, ACh release at the *leaner* NMJ is investigated and compensatory expression of non- $Ca_v2.1$ channels is compared with that found at NMJs of phenotypically similar $Ca_v2.1$ -KO mice.

Ca_v2.1-KO

In view of the importance of the CACNA1A gene, several groups have generated $Ca_v2.1$ -KO mouse strains (Jun et al., 1999; Fletcher et al., 2001; chapter 7). Homozygous animals show

normal development until P10 when symptoms of dystonia, spasms and seizures become obvious. Animals usually die around weaning age, although some animals were reported to have successfully aged under special care (Fletcher et al., 2001). Slowed maturation of CGCs and the persistent expression of tyrosine hydroxylase in deep cortical areas are indicative of impaired brain maturation. These homozygous $\text{Ca}_v2.1\text{-KO}$ mice initially have a normal cerebellar cytoarchitecture, but develop severe progressive cerebellar degeneration (Jun et al., 1999; Fletcher et al., 2001). Cultured primary neurones (both CGCs and PCs) from $\text{Ca}_v2.1\text{-KO}$ mice showed drastically reduced total current densities and compensatory up-regulation of both $\text{Ca}_v2.2$ and Ca_v1 channels (Jun et al., 1999). Experiments in hippocampal slices led to the conclusion that fewer channels are available at any given active zone to mediate the Ca^{2+} influx required for neurotransmitter release (Jun et al., 1999). The central calyx of Held synapse is dependent jointly on $\text{Ca}_v2.1$ and $\text{Ca}_v2.2$ channels (Iwasaki and Takahashi, 1998; Inchauspe et al., 2004; Ishikawa et al., 2005). In $\text{Ca}_v2.1\text{-KO}$ mice, neurotransmitter release at the calyx of Held becomes exclusively (>90%) dependent upon $\text{Ca}_v2.2$ channels, which can apparently compensate for the loss of $\text{Ca}_v2.1$ channels up to approximately 70% of wild-type total current magnitude (Inchauspe et al., 2004). A study on neurotransmitter release at NMJs of these mice has revealed a complex compensatory expression pattern of non- $\text{Ca}_v2.1$ channels (Urbano et al., 2003; Pagani et al., 2004; chapter 7).

$\text{Ca}_v2.1\text{-KO}$ mice exhibit a remarkably similar neurological phenotype to *leaner*- $\text{Ca}_v2.1$ mice (see above). Chapter 7 compares the ACh release characteristics of $\text{Ca}_v2.1\text{-KO}$ and *leaner* NMJs.

Modern molecular biological techniques allow the generation of ‘conditional’ KO mice, carrying ‘floxed’ (= flanked with *loxP* sites) alleles of any gene of interest (e.g. Haller et al., 2004). By crossing these mice with effector mice that express the enzyme Cre recombinase in a time- and site-specific manner, ‘conditional’ knock-outs can be generated. The generation of mice carrying a floxed *Cacna1a* allele, and of mice with such allele deleted by Cre recombinase as well as a first analysis of ACh release at their NMJs is described in chapter 8.

Fletcher et al. (2001) describe a reduction of approximately 50% of P/Q-type current and of approximately 20% of total current density in primary cultured CGCs of heterozygote $\text{Ca}_v2.1\text{-KO}$ mice. Also, there have been further reports of altered synaptic transmission in heterozygous $\text{Ca}_v2.1\text{-KO}$ animals (Kato et al., 2004; Luvisetto et al., 2004)

EA2 in humans is caused by (dominant negative) mutations in *CACNA1A* that often cause truncations of the $\text{Ca}_v2.1$ protein (Jeng et al., 2006). This situation may be modelled by heterozygous *leaner* or heterozygous $\text{Ca}_v2.1\text{-KO}$ mice. In chapter 9, ACh release at NMJs of these mice is described in detail, and their potential use as mouse models for EA2 is discussed. Furthermore, the acute effects of the EA2 drug acetazolamide on ACh release at the NMJ are tested.

FHMI R192Q KI

In the mid-nineties, the Leiden Migraine Genetics Group discovered that mutations in the *CACNA1A*-encoded $\text{Ca}_v2.1$ channel underlie FHMI (Ophoff et al., 1996). One of the mutations, R192Q, eliminates a conserved positive charge within the amphipathic helix IS4, which is one putative voltage-sensor of Ca_v channels (Armstrong and Hille, 1998).

The electrophysiological effects of this mutation have been studied in detail in various model systems. Introduced into rabbit α_{1A} cDNA and expressed in *Xenopus* oocytes, the mutation did not have any effect on channel gating (Kraus et al., 1998). However, measurements in human embryonic kidney cells (HEK293) transfected with the R192Q-mutated human α_{1A-2} isoform of $\text{Ca}_v2.1$ increased maximal current density and larger open probabilities

across a broad voltage range (Hans et al., 1999). In contrast, single channel unitary currents as well as inactivation kinetics remained unaffected. In a HEK tsA-201 cells expression system, G-protein-mediated inhibition was reduced by the R192Q mutation (Melliti et al., 2003). This phenomenon was explained by a putative effect of the mutation on $G\beta\gamma$ protein binding and a resultant facilitation in channel gating.

Chapters 2 and 3 describe the generation and basic neurophysiological characterisation of R192Q KI mice, and the detailed analysis of neuromuscular synaptic transmission in these mice, respectively.

FHM1 S218L KI

The FHM1 mutation S218L was identified in both an Australian and a British family that presented with FHM and symptoms of coma and ataxia (Kors et al., 2001). Patients suffer from delayed severe cerebral oedema and coma triggered by minor head trauma. Other symptoms include ataxia and cerebral and/or cerebellar atrophy (Fitzsimons and Wolfenden, 1985; Kors et al., 2001). Molecular genetic analysis revealed a cytosine to tyrosine change at nucleotide 928 of the CACNA1A gene, causing a hydrophilic serine to be replaced by a hydrophobic leucine residue. Tottene et al. (2005) studied the effects of the S218L mutation both in transfected HEK293 cells, and in primary CGCs obtained from $Ca_v2.1$ -KO mice transfected with S218L mutated- $Ca_v2.1$ and accessory subunits. Mutated $Ca_v2.1$ channels had a similar conductance as wild-type and exhibited a negative shift of activation voltage, thereby causing an increased open probability across a broader voltage-range. Steady-state inactivation appeared normal in S218L-transfected neurones, however, the fast and slow inactivation components were changed (Tottene et al., 2005). The slow inactivation component was increased, whereas fast inactivation occurred more rapidly, explaining increased channel inactivation during short depolarisations and reduced channel inactivation during long depolarisations (Tottene et al., 2005). A reduction in $Ca_v2.1$ mediated current density was found but explained as a likely artefact of overexpression (Tottene et al., 2005; cf. chapters 2 and 3). In chapter 4, the generation and detailed NMJ analysis of FHM1 S218L KI mice are described.

Ducky

Ducky mice carry a genomic rearrangement disrupting the gene encoding the $\alpha_2\delta$ -2 subunit of Ca_v channels, *Cacna2d2* (Barclay et al., 2001). Homozygous *ducky* mice suffer from severe ataxia, a wide-open gait, spike-wave discharges, paroxysmal dyskinesia and CNS dysgenesis (Snell, 1955; Meier, 1968; Barclay et al., 2001). The $\alpha_2\delta$ -2 protein is one of four $\alpha_2\delta$ subunits of Ca_v channels identified to date (Ellis et al., 1988; De Jongh et al., 1990; Williams et al., 1992; Klugbauer et al., 1999; Qin et al., 2002). Interestingly, $\alpha_2\delta$ -2 is, besides $\alpha_2\delta$ -1, the only member of the $\alpha_2\delta$ subunit family to possess a binding site for the anti-convulsant gabapentin (1-(aminomethyl)cyclohexane acetic acid; Neurontin), making it a candidate for conveying the effect of gabapentin (Marais et al., 2001; Qin et al., 2002). The duplication of a non-functional reading frame, underlying the *ducky* mutation, gives rise to two possible mutant constructs in homozygous *ducky* mice, only one of which is translated into protein (Brodbeck et al., 2002). This transcript (termed “du-mut1 α_2 ”) lacks most of the α_2 subunit and the δ subunit, which includes the transmembrane domain (Barclay et al., 2001) and the gabapentin binding site, and can therefore be regarded as a functional KO. The $\alpha_2\delta$ -2 subunit is expressed widely in brain, kidney and testis (Barclay et al., 2001; Brodbeck et al., 2002; Klugbauer et al., 2003). Especially in the cerebellum, $\alpha_2\delta$ -2 expression is high. In *ducky*, dendritic arboration is severely reduced and exhibits weeping willow dendrites and dendritic

thickening (Brodbeck et al., 2002). These morphological aberrations, however, do not affect the number of PC bodies, which is at a level similar to wild-type. Furthermore, no compensatory expression of other $\alpha_2\delta$ subunits has been found (Barclay et al., 2001). Co-expressed with $\text{Ca}_v2.1$ channels and β_4 subunits in *Xenopus* oocytes, $\alpha_2\delta-2$ enhances amplitudes and causes a negative shift in activation voltage (Barclay et al., 2001). Single channel biophysical properties measured in transfected Cos7 cells were unaffected by co-expression with $\alpha_2\delta-2$ (Brodbeck et al., 2002). It has, therefore, been suggested that the $\alpha_2\delta-2$ subunit modulates Ca_v channel function by affecting protein trafficking and/or turnover, rather than by changing single channel properties directly (Brodbeck et al., 2002). In line with this finding, measurements in primary dissociated PC neurones showed an approximately 35% reduction in P-type currents in *ducky* mice compared with wild-type (Barclay et al., 2001).

The neurological phenotype of *ducky* mice resembles that of many other Ca^{2+} channel mutants, especially with respect to the spike-wave discharges, which are also present in *tottering*, *lethargic* and *stargazer* mice (Noebels and Sidman, 1979; Noebels et al., 1990; Hosford et al., 1992; Barclay et al., 2001). However, no information is available to date regarding the role of $\alpha_2\delta$ subunits in transmitter release at CNS synapses or at the NMJ. Chapter 10 presents a characterisation of ACh release at the NMJ of *ducky* mice.

Lethargic

Lethargic mice arose spontaneously in 1962 and were identified on the basis of a severe neurological phenotype, consisting of chronic (mild) ataxia, hypoactivity and intermittent attacks of severe paroxysmal dyskinesia (Dickie, 1964; Dung and Swigart, 1971; Dung and Swigart, 1972; Burgess et al., 1997; Khan and Jinnah, 2002). Electroencephalography showed discharges suggestive of absence epilepsy. The phenotype sets on around P10, with a critical period between P15 and 2 months of age, during which homozygous *lethargic* mice have lower body weights, increased lethality and suffer from severe lymphocytopenia (Dung and Swigart, 1971; Dung and Swigart, 1972). Animals which survive this period can live to normal age but have reduced fertility (Dung, 1977). The *lethargic* locus has been identified as the *Cchb4*-encoded β_4 subunit of Ca_v channels (Southard, 1973; Chin et al., 1995; Burgess et al., 1997), which is a homologue of the human CACNB4-encoded β_4 subunit (Escayg et al., 1998). The mutation (a four nucleotide insertion in the 5' splice site) is predicted to result in a truncated protein, however, detailed analyses have failed to detect any β_4 protein (McEnery et al., 1998) in *lethargic* mice. Thus, *lethargic* mice can essentially be considered a functional knock-out for the β_4 subunit of Ca_v channels. Early studies have implicated GABA_B receptors in the generation of seizures. An increased presence of GABA_B receptors was identified in *lethargic* mice that correlated with increased seizure frequency (Lin et al., 1993; Lin et al., 1995), and linked to thalamic regions (Hosford et al., 1995). Interestingly, recordings from thalamocortical slices of *lethargic* brain showed a significant increase in total LVA Ca^{2+} currents compared with wild-type. This increase might cause abnormal thalamocortical synchronisation and result in absence epilepsy (Zhang et al., 2002).

To date, four β subunits of Ca_v channels have been identified (for review see Catterall, 2000; Dolphin, 2003). They can interact with pore-forming α_1 subunits of HVA Ca^{2+} channels via a highly conserved α_1/β interaction site, consisting of an 18 amino acid motif with 9 conserved residues on α_1 subunits, and a highly conserved motif of 30 amino acids on the β subunit (De Waard et al., 1994; Pragnell et al., 1994; De Waard et al., 1995).

Many studies have focused on the question, whether α_1 subunits of Ca_v channels associate with other β subunits in the absence of β_4 . Total expression levels of β subunits in *lethargic* brain were reported to be reduced, whereas expression of the β_{1b} subunit was

increased in fractions of both forebrain and cerebellar membranes (McEnery et al., 1998). Interestingly, the expression level of $\text{Ca}_v2.2$ channels was reduced in *lethargic* cerebellum, a region associated with high β_4 subunit expression in wild-type (McEnery et al., 1998). In the forebrain, where β_3 subunits are the most abundant species, expression of the β_{1b} subunit was increased, whereas binding to $\text{Ca}_v2.2\text{-}\alpha_1$ subunits remained at similar levels in the cerebellum (McEnery 1998). However, in a similar study Noebels and colleagues did not identify a reduction in $\text{Ca}_v2.1$ or $\text{Ca}_v2.2$ channels, but an increased incorporation of other β subunits, a process termed “reshuffling” (Burgess et al., 1999). Measuring KCl-induced Ca^{2+} uptake into neocortical synaptosomes, the ω -agatoxin-IVA sensitive $\text{Ca}_v2.1$ channel contribution was significantly reduced (Lin et al., 1999). In contrast, P-type currents in *lethargic* were identical to those measured in wild-type cerebellum (Burgess et al., 1999). The only synaptic studies of *lethargic* to date revealed a large reduction in glutamatergic (excitatory), but not GABAergic (inhibitory) neurotransmission in *lethargic* thalamic neurons (Caddick et al., 1999) and normal pre-synaptic Ca^{2+} influx at the hippocampal CA3-CA1 synapse (Qian and Noebels, 2000). Taken together, it appears that there is only limited functional redundancy of β subunits in some parts of the CNS (Burgess et al., 1999). Of interest, mice deficient for the β_3 subunit of Ca_v channels are phenotypically normal, despite complex compensatory mechanisms involving α_1 and β subunits (Namkung et al., 1998).

To date, only one report has focused on the localisation of accessory subunits at the mouse NMJ (Pagani et al., 2004). It appears that the predominant subunit at the mouse NMJ is β_4 , with smaller amounts of β_{1b} and β_{2a} , but not β_3 , subunits present. Of interest, ablation of the $\text{Ca}_v2.1$ channel in $\text{Ca}_v2.1\text{-KO}$ mice did affect neither distribution nor expression levels of β subunits at the NMJ (Pagani et al., 2004). Chapter 10 describes neurotransmitter release at the NMJ of *lethargic* mice.

Stargazer

Named after their unusual head tossing movement, *stargazer* mice were first described in 1990 (Noebels et al., 1990) as exhibiting ataxia, paroxysmal dyskinesia, vestibular dysfunction and spike-wave discharges indicative of absence epilepsy in humans (Noebels et al., 1990; Khan et al., 2004). The mutation underlying *stargazer* was identified as an early transposon insertion in the second intron of the *Cacng2* gene (Letts et al., 1997; Letts et al., 1998), resulting in the complete loss of the *Cacng2*-encoded protein, named *stargazin* (Sharp et al., 2001).

The *stargazin* protein product shows 25% amino acid identity with the γ subunit of Ca_v channels, has a similar structure consisting of four transmembrane domains with cytoplasmic termini, and could successfully modulate $\text{Ca}_v2.1$ channel kinetics in a heterologous expression system (Letts et al., 1998). Based upon these results, *stargazin* was classified as novel γ_2 subunit of Ca_v channels.

Controversy has, however, arisen over the role of *stargazin* as a modulator of Ca_v channels following several studies failing to show effects of *stargazin* on Ca_v in heterologous expression systems (for review see Letts, 2005). Interestingly, recordings from thalamocortical slice preparations showed that both HVA and LVA activity was altered in *stargazer* brain, in a similar fashion as in *tottering* and *lethargic* preparations (Zhang et al., 2002) supporting a role as modulatory subunit of Ca_v channels. Studies into the ataxic phenotype of *stargazer* revealed a plethora of cerebellar defects (Letts, 2005). Whilst cerebellar morphology appeared largely normal, CGC specific deficits have been reported (Qiao and Meng, 2003). These include loss of functional α -amino-3-hydroxy-5-methyl-4-isoxazolepropionic acid (AMPA) receptors in granule cells, lack of brain-derived neurotrophic factor and a reduction

in GABA_A receptor α_6 and β_3 subunits (Thompson et al., 1998; Hashimoto et al., 1999; Chen et al., 1999). Nicholl and colleagues later found that *stargazin* is required for trafficking of AMPA receptors through the Golgi to the plasma membrane and the anchoring of receptors at the post-synaptic membrane (Chen et al., 2000; Schnell et al., 2002; Dakoji et al., 2003). Recently, *stargazin* has been suggested to act as a cell adhesion molecule, resulting from its structural similarity with members of the claudin family and its early embryonic expression pattern (Letts et al., 2005; Price et al., 2005). Chapter 10 studies the effects of the absence of *stargazin* on ACh release at *stargazer* NMJs.

Aims and Outline of this Thesis

This thesis aims at characterising the effects of mutations in pre-synaptic Ca_v2.1 channels on (neuromuscular) synapse function. Understanding the synaptic effects of these mutations is expected to contribute to our understanding of the pathophysiology of the complex human disorders (thought to be) associated with Ca_v2.1 channel dysfunction.

Using knock-in technology, the first animal model for FHM was generated in Leiden, carrying the FHM1 R192Q mutation in *Cacnala*. **Chapter 2** describes the generation and neurophysiological analysis of these R192Q KI mice, including studies on primary cultured cerebellar neurones, a basic analysis of ACh release at the NMJ and CSD measurements. The subsequent chapter provides a more detailed electrophysiological and morphological characterisation of neuromuscular synaptic abnormalities in these mice (**chapter 3**). Mice that were heterozygous for the R192Q mutation were studied in order to assess a possible gene-dosage effect. Furthermore, a quantification of ultra-structural NMJ parameters, *in vivo* EMG measurements and investigation of neurotransmitter release in aged animals (in order to assess a possible progressiveness of changes) are described.

Chapter 4 is a detailed account on electrophysiological NMJ abnormalities found in FHM1 KI mice carrying the *Cacnala* S218L mutation, causing FHM with increased susceptibility to brain oedema and coma in patients.

The subsequent chapters centre on neuromuscular synaptic transmission in the natural *Cacnala* mutants *tottering* (**chapter 5**), *rolling Nagoya* (**chapter 6**) and *leaner* (**chapter 7**). In contrast to the FHM1 KI mutant mice, these strains exhibit more severe neurological phenotypes, muscle weakness (*rolling Nagoya*) or compensatory expression of non-Ca_v2.1 channels (*tottering*, *leaner*). The compensatory expression profile of non-Ca_v2.1 channels in the phenotypically similar *leaner* and Ca_v2.1-KO mice is characterised and compared in **chapter 7**.

For our understanding of Ca_v2.1 channel function, it is interesting to study the effects of the ablation of the Ca_v2.1 protein in a time- or site-specific manner ('conditional Ca_v2.1-KO'). **Chapter 8** describes the generation and ACh release analysis at the NMJ of mice carrying a floxed *Cacnala* gene, before and after its deletion with Cre recombinase, thereby providing the basis for the generation of spatiotemporally conditional Ca_v2.1-KO mice.

CACNA1A mutations present in EA2 often cause a truncated Ca_v2.1 protein with possible dominant negative effects on channel function. Heterozygous *leaner* or Ca_v2.1-KO mice may model this condition. In **chapter 9**, ACh release at their NMJs, and the possible effects of the EA2 drug acetazolamide thereupon, have been studied.

Ca_v2.1 channels have accessory subunits, which can modulate the function and/or expression level of the channel *in vitro*. *Ducky*, *stargazer* and *lethargic* mice lack the functional subunits $\alpha_2\delta$ -2, β_4 and γ_2 , respectively. **Chapter 10** presents the characterisation of

ACh release at NMJs of these mice, in order to assess the contribution of accessory subunits to neurotransmitter release.

Topiramate is an anti-convulsant drug that has recently become successfully employed in migraine prophylaxis. Modulation of Ca_v2.1 channel function has been proposed as one possible mechanism of action of topiramate. To test this hypothesis, the effects of acute application of topiramate on ACh release at the NMJs of FHM1 R192Q KI and *tottering* mice have been investigated (**chapter 11**).

A general discussion of the findings presented in this thesis and suggestions for future research are given in **chapter 12**.

